Effects of electric charges on hydrophobic forces. II.

D. Bulone,[1] V. Martorana,[1] P. L. San Biagio,[1] and M. B. Palma-Vittorelli[2,*]
[1]*CNR Institute for Interdisciplinary Applications of Physics, Via U. La Malfa 153, I-90146 Palermo, Italy*
[2]*INFM and Department of Physical and Astronomical Sciences, University of Palermo, Via Archirafi 36, I-90123 Palermo, Italy*
(Received 18 February 2000)

We study by molecular-dynamics simulations the effect of electric charges of either sign on hydrophobic interactions and on the dynamics of hydration water, using explicit water and very simplified solutes. Results show that the presence of a charged solute can disrupt the ''hydrophobic contact bond'' between two apolar solutes nearby, by forcing them towards a different configuration. As a consequence of different structural changes of the solvent caused by charges of opposite sign, the effect is markedly charge-sign-dependent. Analogous weaker effects appear to be induced by the presence of one additional apolar element. The dynamics of hydration water around each solute is also seen to be strongly influenced by the presence of other (charged or uncharged) nearby solutes. Comparison between our results on hydration water dynamics around charged solutes and available experimental data allows sorting out the effects of solute charge sign and size. Our results also offer a plain interpretation of the equivalence of the effects on water structure due to solute ions and to high pressures. These results reflect at a basic paradigmatic level the immensely more complex cases of well-known phenomena such as salting-in and salting-out, and of protein conformational changes caused, e.g., by the arrival of a charged or of an apolar group (phosphorilation or methylation). As it will be discussed, they help in the direction of Delbruck's desirable ''progress towards a radical physical explanation'' for this class of phenomena.

PACS number(s): 82.30.Nr, 02.70.Ns, 61.20.Ja, 82.20.Wt

I. INTRODUCTION

Electrostatic forces are known to play important biological roles such as in biomolecular structure, recognition, and function. However, generalized forces resulting from the interaction of solutes with the solvent, and related to the thermodynamic drive towards a decrease of the overall free energy of hydration, play an equally important role, due to their large and sometimes overwhelming size. Hydrophobic interactions are the best known example of such solvent-induced interactions, and have been the object of a vast amount of theoretical, experimental, and simulation work [1–10]. Hydrophobic forces have, with good reason, been taken as the paradigm of solvent-induced forces (SIFs) and of their special feature of acting even among solutes which would not interact *in vacuo*. However, recent results [11–14] indicate that it would be unproductively limiting to restrict the rich phenomenology of SIFs to the case of hydrophobic forces (taken as additive). One reason for this is that hydrophobic forces are only a subset of SIFs. Another reason lies in the inherently strong nonadditivity of SIFs, which makes them strongly dependent upon the actual spatial context of the whole system of surrounding solutes and solute elements [11–14]. General features of hydration, of related solvent-induced interactions, and of the potential of mean force (PMF) can be studied in the case of complex solutes by computer-efficient methods based on pair expansion [Kirkwood's superposition approximation (KSA)] [15], triplet expansion, and proximity approximation of the many-body correlation function [16–19] or on continuum modeling of the solvent [20]. In the case of biomolecules, these methods prove adequate for relatively coarse-grained studies. However, they may miss all-important details on the microscopic scale, such as SIFs acting on individual residues along directions opposite to those expected on the basis of their hydrophobic/philic character [12]. (Such sign inversion does not need to appear paradoxical, if viewed in terms of Anfinsen's [21] remark that the equilibrium situation must correspond to a minimum of the free energy of the entire system.) Departures from expectations based on coarse-grained simplifications can be, of course, highly relevant to the specificity of bimolecular interactions. The complementary approach of using supersimplified model solutes and explicit molecular modeling of the solvent enables taking into account interactions to all orders, responsible for the mentioned unexpected local features. This approach has enabled us to elicit the inherently strong nonpair additivities and related context dependence and long-range correlated action of solvent-induced interactions [11–14]. Also, it has shown how solvent-induced interactions can transform flat configurational potential-energy landscapes of simple solutes in PMF landscapes that allow for stable and unstable configurations not existing *in vacuo* [22]. In this way, the basic essence of solute-solvent dynamic coupling has also been visualized [22]. These effects are relevant to the case of complex solutes, such as macromolecules, where each element undergoes solvent-induced interactions with many other elements at close distance.

A recent interesting study [23] of hydrophobic hydration and interactions combines molecular-dynamics (MD) simulations of *N*-acetyl-leucine-amide (NALA) in explicit water with neutron-scattering experiments on its aqueous solutions. This has allowed sorting out the solute-solute pair distribution function which, notwithstanding the low concentration

*Corresponding author. FAX: +39.091.617 3895. Email address: Vittorel@iaif.pa.cnr.it

used, exhibited a solvent-separated minimum and possibly longer-ranged correlations. These results agree with MD studies of a protein in water, showing the existence of extended H-bonded networks promoted by solutes and encompassing distances up to a few nanometers, as revealed by correlations among time-resolved SIFs acting on even distant amino acids [12].

All that shows the interest of approaching the complexity of solvent-induced interactions through the study of a number of elementary paradigms or ''morphemes.'' The present MD study concerns the effect of electric charges on the (hydrophobic) SIFs acting on two supersimplified apolar (uncharged) solutes. By definition, apolar solutes do not interact *in vacuo* with electric charges. Consequently, any change of SIFs acting between them, observed when an electric charge is added to a third nearby solute, can be uniquely traced to changes of the probability of the occurrence of configurational states of the solvent, caused by the electric charge. The joint use of very simplified solutes and of explicitly and realistically modeled solvent molecules enables here sorting out the very basic mechanism of modulation of hydrophobic SIFs by an electric charge.

Partial results have already been reported [14] showing a marked charge-sign dependence of modulations of hydrophobic forces by electric charges. This effect, which agrees with the known different response of the aqueous medium to perturbations caused by opposite electric charges [24], was traced to the nonsymmetric distribution of charges on the water molecules [13,14]. Here we present the effect of charges of both signs on two inter-related aspects of hydrophobic interactions. These are the PMF between apolar solutes and the dynamics of hydration water. We show how in the presence of an electric charge the so-called hydrophobic contact can become unfavorable and how this dramatic effect on the PMF is related to the increase of the configurational lifetime of hydration water.

Solvent-induced interactions are expressed in terms of hydration, and more quantitatively in terms of hydration free energy, G_{SW} (where S and W stand for solute and water, respectively), and SIFs. As a consequence of excluded volume and interaction potential, solutes alter the configurational landscape of the potential energy of water and therefore the statistically relevant water configurations (hydration) and their potential energy, multiplicity, and related connective paths. This causes corresponding changes of configurational lifetime and free energy, G_{SW} (hydration free energy). The effect of a solute on the energy landscape of water already perturbed by other solutes cannot be expected to be the same as in their absence, and it will depend upon solute-solute distances and mutual configurations. Therefore, whenever hydration regions of solutes overlap [25], the free energy and configurational lifetime of hydration around individual solutes will depend upon the spatial distribution of all other solutes, that is, it will be ''context-dependent.'' Accordingly, the total free-energy change caused by n solutes can be written as

$$G_{\mathrm{SW}}(1,2,\ldots,n)=\sum_{i}^{n} G_{\mathrm{SW}}^{(1)}(i)+\sum_{i<j}^{n} \delta G_{\mathrm{SW}}(i,j) + \cdots + \sum_{i<j<\cdots}^{n} \delta G_{\mathrm{SW}}(i,j,\ldots,n). \quad (1)$$

As a consequence of the dependence of the second- and higher-order terms upon the mutual configuration of solutes, a SIF (indicated by $F_{\mathrm{SI},k}$) acts on each solute, given by

$$F_{\mathrm{SI},k}=-\mathrm{grad}_k G_{\mathrm{SW}}(1,2,\ldots,n). \quad (2)$$

Third- and higher-order terms in Eq. (2) are responsible for nonadditivity of SIFs. As already shown [11–14], these terms are not small perturbations, being inherently comparable with or larger than second-order ones.

SIFs acting on a fixed solute, k, can equivalently be viewed as the thermodynamic average of the total force exerted on a solute by all water molecules in the bath:

$$F_{\mathrm{SI},k}=\left\langle \sum_{W} \mathbf{F}_{wk} \right\rangle, \quad (3)$$

where $\mathbf{F}_{wk}$ is the force vector exerted by each water molecule on solute k, the sum is over all water molecules, and the angular brackets express a thermodynamic average [15]. Instantaneous values of the force exerted on a solute by water molecules in a particular configuration are provided by each term $\Sigma_w \mathbf{F}_{wk}(t)$, and time-resolved features of this force reflect the dynamics of water [26,11–14]. The nonzero value of its thermodynamic average is a consequence of the inhomogeneous spatial average distribution of water molecules, caused by the interaction with the given nonspherical solute system. In Kirkwood's approach [15], the solvent contribution to the potential of mean force, Ψ, is implicitly defined as

$$F_{\mathrm{SI},k}=-\mathrm{grad}_k \Psi(1,2,\ldots,n) \quad (4)$$

which is coincident with Eq. (2). The total PMF (Ω) and the total force acting on each solute are

$$F_{\mathrm{total},k}=F_{\mathrm{dir},k}+F_{\mathrm{SI},k} \quad \text{and} \quad \Omega=U+\Psi, \quad (5)$$

where U and Ψ are the direct and solvent-induced contributions, respectively. The PMF can be expressed in terms of the n-body solute-solute correlation function as

$$\Omega(1,2,\ldots,n)=-kT \ln g^{(n)}(r_1,r_2,\ldots,r_n). \quad (6)$$

The above equations cover the intrinsic many-body nature of the PMF, and show how the validity of a pairwise approximation depends on the factorizability of $g^{(n)}(r_1,r_2,\ldots,r_n)$.

In what follows, we report results of MD simulations on a model system. Sufficiently long runs assure statistical significance. We compute SIFs in a set of solute configurations, sufficiently ample to obtain Ψ from Eq. (4) by numerical integration. We study how the interaction between two hydrophobic solutes and the dynamics of the hydration water are influenced by the presence of a third solute which, *ceteris paribus*, can be in turn electrically neutral, positively, or negatively charged. Subtraction of the effects of a neutral solute (which also includes that due to a cavity in a simple solvent) and of contributions due to the action of electric charges in a hypothetical continuum dielectric solvent enables us to sort out the role of the rearrangements of the H-bond network caused by the electric charges of either sign. Data show that the presence of a charged solute (particularly in the case of negative charge) can destabilize hydrophobic

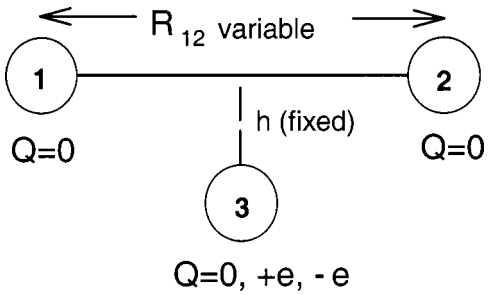

FIG. 1. Three-solute configuration used in the present work. In each run solutes are kept fixed. Different runs correspond to different center-to-center distances R_{12}, while in all cases it is $h = 3.86$ Å. All solutes are Lennard-Jones spheres, with $\in$ and σ parameters as those of the water's oxygen. Solute 3 can bear a null, positive, or negative unitary electronic charge.

interactions to such an extent that contact and solvent-separated solute configurations of two hydrophobic solutes can become less favorable than infinite-distance ones. Equivalently, they show that electric charges can destroy so-called ''hydrophobic bonds.'' We note that our simple system can be thought to mimic two solute elements, such as two hydrophobic residues, at relatively close distance in the spatial context of a whole protein. This suggests that the present results should be borne in mind when attempting a deeper understanding of experimental facts, such as the effects of salts (salting-out and salting-in) and those due to phosphorilation and methylation. Also, our results can be consistently related to recent experimental data concerning the equivalence of the effects of ions and of high pressure on water structure [27].

Time-resolved features of SIFs and residence times of hydration water elicited in the present case show how dynamical features of hydration of one solute can heavily depend upon the presence and character of other solutes, in agreement with the strong many-body character of SIFs and PMF in aqueous solutions. Such dynamical features and, specifically, residence and structural relaxation times are particularly relevant to transport properties [28] involved, in turn, in kinetic aspects of a variety of biologically relevant processes.

II. MODEL SYSTEM AND COMPUTATIONAL DETAILS

Our system contained three solutes, modeled as Lennard-Jones (LJ) spheres, in a bath of explicit molecular water. We used solute configurations such as in Fig. 1, where solutes 1 and 2 remain in all cases electrically uncharged and solute 3 can either be uncharged or bear a unit electronic charge of either sign. The value of the h distance is kept fixed at 3.86 Å, while different R_{12} values are selected in the range 3.4–14 Å for different MD trajectories. The $h = 3.86$ Å value is such that when solutes 1 and 2 are in contact, the $R_{13} = R_{23}$ distance corresponds to a strong (and strongly variable with the distance) value of SIFs between solutes 1–3 and 2–3. When appropriate, the total charge was neutralized by an evenly distributed charge density of opposite sign. Runs with single solutes or in the absence of solute 3 were also performed.

The size of the simulation box changed in accordance with the value chosen for the R_{12} distance, so as to allow at least three layers of water molecules between solutes and the box walls. Accordingly, the number of water molecules varied from 343 to 539. The water-water potential was TIP 4P [29], which is particularly suitable for ion-water solutions. In all cases, the LJ parameters of the solute-solute and solute-solvent potential were the same as for the water oxygen, that is, $\varepsilon = 0.648\,57$ kJ mol^{-1} and $\sigma = 3.154$ Å.

The thermodynamic ensemble was NVE, $T = 298$ K, and density 1 gr cm^{-3}. Periodic boundaries and Ewald sums were used. The MD runs were performed using a modified (leap-frog) Verlet algorithm [30] with a 2-fs time step. Independent trajectories of 800–1200 ps were run for each solute configuration, following 200-ps equilibration. For better statistical significance, total composite trajectories were obtained as sequences of 200-ps trajectories decoupled from each other by 20-ps annealings at 800 K, followed by 40-ps equilibration at 298 K.

SIFs on solutes 1 and 2 at each R_{12} distance were computed as time averages (along the whole composite trajectory) of the instantaneous force vectors exerted on the solute by all water molecules [26]. Direct solute-solute (LJ) forces were separately taken into account when appropriate. This was repeated for about 15 values of the R_{12} distance evenly spaced between 3.4 and 14 Å, that is, in the whole range from below the minimum of the direct LJ potential to negligible direct and solvent-induced interactions.

Information on the dynamic properties of hydration water was obtained from the residence time of the water molecules in the first hydration shell. To define the shell, we used a cutoff distance from the solute, R, having a selected value close to the first minimum, R_0, of the solute-solvent correlation function $g(r)$. Residence times were derived using a two-value variable $p_j(t,t+\tau)$ defined for each jth water molecule. Its value was 1 if the jth molecule remained in the first hydration shell for the entire interval t, $t+\tau$, and 0 otherwise. A time-correlation function averaged over all molecules and along the whole trajectory was obtained as

$$P(\tau) = \sum_j \sum_t p_j(t,t+\tau) \tag{7}$$

and its decay time gave the average residence time τ_{res} in the first hydration shell [31].

III. RESULTS AND DISCUSSION

Our solute configuration is in Fig. 1, as already described. In Figs. 2 and 3 we report results on forces acting on solutes 1 and 2 and related PMF [total, direct, and solvent contributions, as per Eq. (5)], respectively, in four different situations. These are indicated as (i) 2LJ (solute 3 absent); (ii) 2LJ+LJ (solute 3 present but uncharged), (iii) 2LJ+Q^+ (solute 3 bearing one positive electronic charge); and (iv) 2LJ+Q^- (solute 3 bearing one negative electronic charge). In Fig. 2, the total force component acting on solute 1 or (given the symmetry) on solute 2 (top panel) along the R_{12} direction and the solvent contribution to this force (that is, SIF, bottom panel) are shown for different values of R_{12}. It is seen that, with respect to case (i), in case (ii) the SIF is markedly different. When a charge is added to solute 3, SIFs between solutes 1 and 2 are strongly enhanced in the

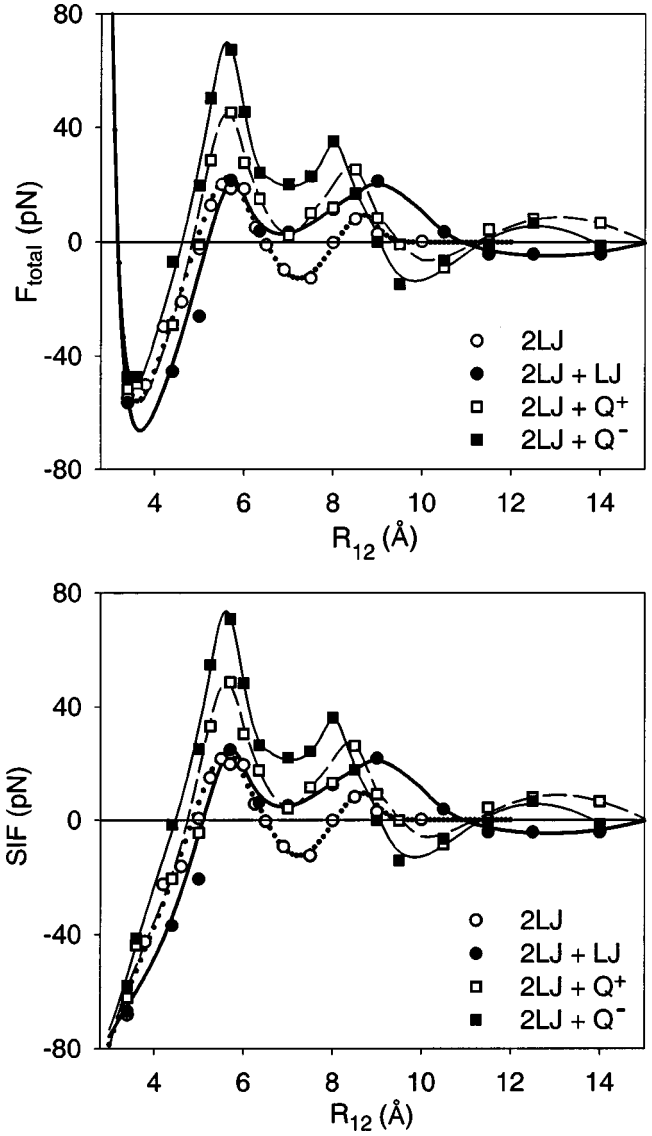

FIG. 2. Force component acting on solutes 1 and 2 along the R_{12} direction, for different values of the R_{12} distance and different conditions of solute 3 as defined for Fig. 1. Top, total force. Bottom, solvent-induced contribution (SIF). Lines connecting data points are polynomial best fittings. Symbols: (i) empty circles, 2 LJ (solute 3 absent); (ii) full circles, 2 LJ+LJ (solute 3 uncharged); (iii) empty squares, 2 LJ+Q^+ (solute 3 positively charged); (iv) full squares, 2 LJ+Q^- (solute 3 negatively charged).

repulsive (positive) range, the more so in the case of the negative charge. This agrees with the partial results reported in [14]. However, new and valuable information comes now from PMF curves shown in Fig. 3. These curves are obtained by fitting SIF data points to a polynomial function and by integrating the latter over the R_{12} distance. The total PMF, the direct solute-solute potential, U, and the solvent-induced contribution, Ψ, are shown in the top, central, and bottom panel, respectively. In the absence of a third solute, two negative minima of the total PMF are seen, respectively, corresponding to contact and solvent-separated configurations, as expected [6]. Solute 3, even when uncharged, raises the PMF value at the contact minimum. The presence of a charge (either positive or negative) on solute 3 raises this PMF minimum up to positive values, thus making it unfa-

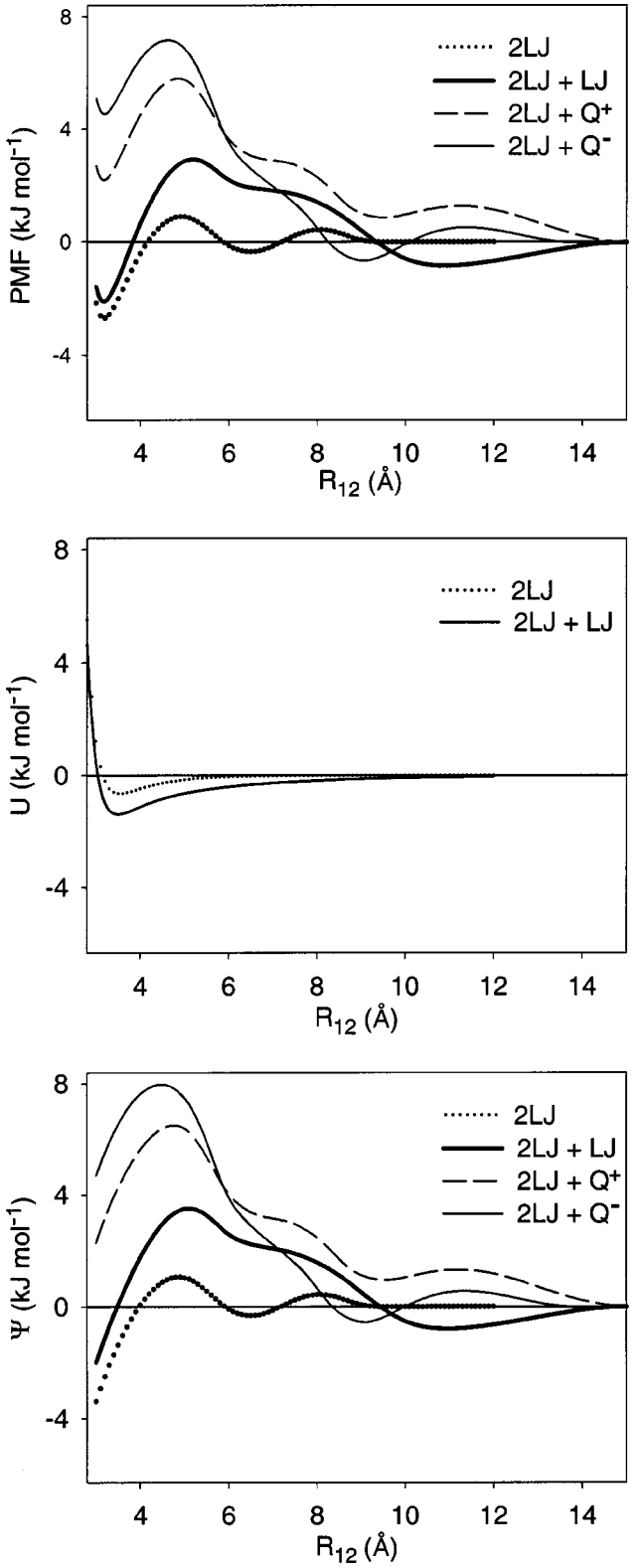

FIG. 3. Potential of mean force (PMF) for solutes 1 and 2 of Fig. 1 under different conditions. PMF is obtained by integration of the polynomial best-fitting lines of Fig. 2. Top, total PMF. Center, contribution of the direct interaction potential, U (charge and solvent independent), in absence (dotted line) and in presence (continuous line) of solute 3. Bottom, solvent contribution to PMF Ψ. Dotted line, solute 3 absent; heavy continuous line, solute 3 uncharged; broken line, solute 3 positively charged; thin continuous line, solute 3 negatively charged.

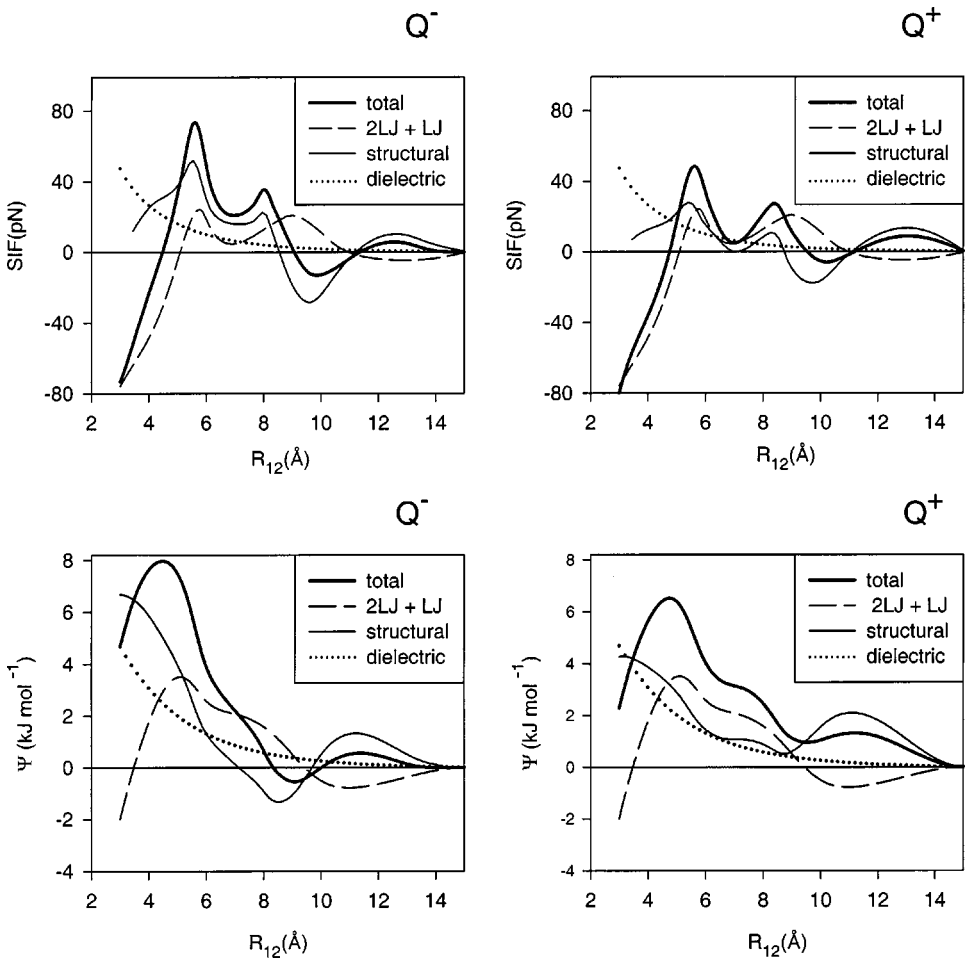

FIG. 4. SIF, and solvent contribution to PMF, Ψ (heavy lines), are decomposed in the following contributions: uncharged solute (broken line), which includes excluded volume and LJ potential interactions; continuum dielectric solvent (dotted line), classically computed, charge-sign-independent; H-bond network perturbation (thin line), obtained by difference. The latter is responsible for the full charge sign dependence. Left, negative charge; right, positive charge.

vorable, relative to large-distance configurations. A favorable, if shallow, solvent-separated minimum, shifted towards higher distances, is present in the case of uncharged and negatively charged solute 3, but not when the latter is positively charged. Sorting out the different contributions to these changes, as done in Fig. 4, helps us understand the origin of these results. Here, the total SIF and Ψ are decomposed in a term caused by the uncharged solute 3 (which includes the cavity contribution), a term which would be caused by an electric charge in a continuum dielectric solvent (analytically calculated in classical terms), and a term (obtained by difference) due to the perturbation of the H-bond network by the electric charge. The latter is seen to be very large or even dominant and is of course responsible for the whole charge-sign dependence. With reference to the SIFs (upper part of the figure), at R_{12} distances up to about 11 Å, this contribution is larger in absolute value for the case of the negative charge, while it becomes somewhat weaker at larger R_{12} values, where total SIFs become constantly weaker. This behavior is reflected in the solvent contribution to the PMF, Ψ, shown in the same figure. The origin and charge sign dependence of the complex behavior of the effects due to perturbation of the H-bond network will become clearer on the basis of the hydration data presented below. For the time being, we conclude that, all in one, the contact hydrophobic pair is destabilized by the presence of our solute 3, when charged, to such an extent that the so-called ''hydrophobic contact'' or ''bond'' does not exist in practice any longer. In the case of negative charge, this effect is more marked, but the long-distance ($\approx$9 Å) solvent-separated configuration may have statistical significance.

Figures 5 and 6 concern resolved features of SIFs, reflecting some dynamic aspects of hydration water. The distribution of SIFs (vectors and intensities) acting on each solute along a MD trajectory is shown in Fig. 5. The larger spread observed around solute 3, when charged, reflects the sensitivity of SIFs to the orientational disorder of water molecules. Such disorder, as expected, has instead no influence on SIFs acting on uncharged LJ solutes. Around a negatively charged solute, the spread is larger as a consequence of the fact that the average solute-solvent interaction is stronger than in the case of positive charge [13,14]. This also agrees with the data of Fig. 6, top, showing that in the Fourier spectra of time-resolved SIFs a well-resolved feature, barely visible in the case of LJ solutes, appears in the cases of charged solutes, with higher resolution and at higher frequency for the negative charge. This shows that in the hydration shell of positively and negatively charged solutes, the dynamics of water molecules acquires a character of localized oscillation, and that the characteristic restoring force of such oscillation is larger in the negative charge case. These data reveal that water molecules in the first hydration shell are more tightly bound to the negatively than to the positively charged solute. This is confirmed and reinforced by the behavior of the solute-oxygen correlation function, $g(r)$, shown in Fig. 6, bottom, and by data in the next figures that we are going to discuss.

In Figs. 7 and 8, we report the effects of solutes and of

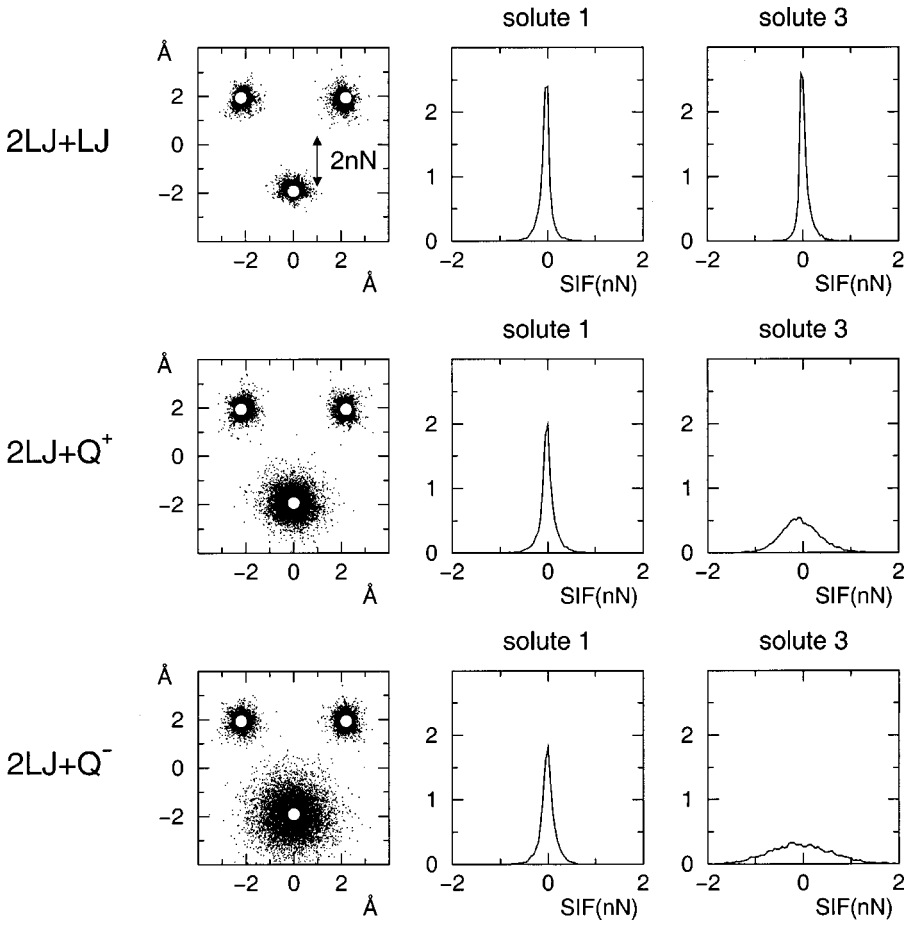

FIG. 5. Distribution of instantaneous forces acting on solutes in a typical case ($R_{12}=4.2$ Å, see Fig. 1). Left column, distribution of traces on the solute plane of the force component acting on each solute. Solute 3 is uncharged (top), positively charged (center), or negatively charged (bottom), respectively. Center column, distribution of intensities of forces acting on solute 1 (or, symmetrically, on solute 2) when solute 3 is uncharged (top), positively charged (center), or negatively charged (bottom). Right column, distribution of intensities of the forces acting on solute 3 when it is uncharged (top), positively charged (center), or negatively charged (bottom), respectively. The ordinate represents the number of configurations ($\times 10^{-3}$). The intensity of the average SIFs is measured in the left and center panels by the offset, along the abscissa, of the symmetry axis of the bell curves relative to zero. This shows that fluctuations can be very much larger than average values [14].

their spatial configuration or ''context'' on the diffusional properties of hydration water molecules. To this purpose, we have computed the residence time, τ_{res}, of water molecules in the first hydration shell of solutes. Water molecules were assumed to be in the first hydration shell if the distance between the water oxygen and the solute center was less than a selected cutoff value, R, chosen in proximity of the first minimum of $g(r)$, R_0. In Fig. 7, we present the residence time of water molecules in the first hydration shell of single ''solutes.'' These are a freely diffusing water molecule in the bath and one single, fixed LJ solute bearing 0, $+1$, and -1 units of electronic charge, respectively. The residence time is evaluated for different R values and plotted as a function of R/R_0. It is seen that the τ_{res} values relative to uncharged and positively charged solutes are very similar to each other and almost three times larger than that relative to pure water. In the case of the negatively charged solute, a further fivefold increase is observed. A useful visualization of residence times of individual hydration molecules is given in the panels of the bottom row. Here each circle represents a particular (numbered) water molecule present in the hydration shell ($R/R_0<1$), so that a time interval in which a molecule resides within the hydration shell turns out to appear as a continuous segment. (For better readability, only the four nearest water molecules are shown in the figure.) Here again the remarkable effect of the negatively charged solute is well visible. The R dependence shown in the top row can be qualitatively understood under the approximation that the probability that a motional event takes a particular water molecule to an (arbitrarily small) elementary cell within the chosen space region should be proportional to the volume of the region. (We must realize, however, that in this approximation we disregard important collective features of structural relaxation mechanisms of water [32].) The probability that the same event takes the molecule across the surface should instead be proportional to the surface area. The residence time can be thought to be proportional to the ratio of these probabilities. This results in a linear increase of τ_{res} versus R, whose slope reflects, on the same qualitative basis, the mean length of the displacement. Following this view, these data show how hydration water in the first shell of the solute is considerably more tightly restrained in the case of the negatively charged solute than in the cases of positive or null charges, in agreement with the conclusions suggested by the time-resolved features of SIFs and by the $g(r)$ (Figs. 5 and 6). Notably, this trend is reversed for $R/R_0>1$. The observed R dependence suggests that the motion of water molecules be closer to a Levy flight than to a random walk, despite the fact that it is expected to be much more complex than either. One reason for that is the mentioned collective (or at least strongly correlated) nature of these motions [32]. Also, it has to be noted that, due to this collective nature, the comparison of τ_{res} values relative to different solutes is more meaningful than that relative freely diffusing water molecule.

Residence time data taken with a cutoff distance $R/R_0=1$ relative to solute pairs and to the three-solute configuration of Fig. 1 are presented in Fig. 8 versus the R_{12} center-to-center distance. In the two-solute configuration (top row), solute 3 is absent and solute 1 is either uncharged or posi-

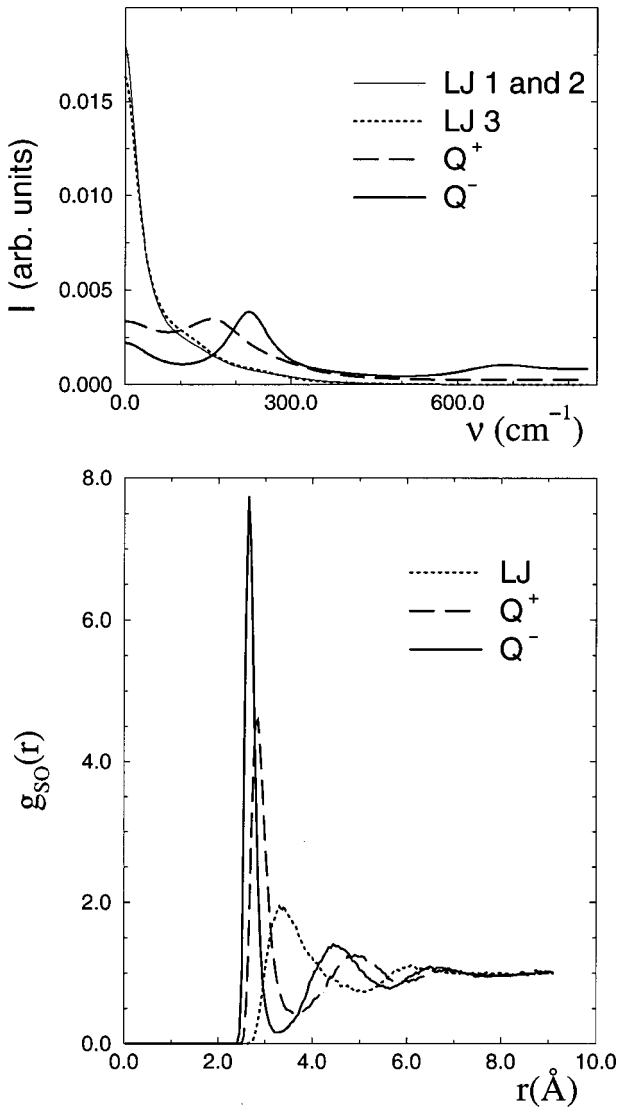

FIG. 6. Top, normalized Fourier spectra of SIFs, acting on solutes, in the configuration of Fig. 1, at $R_{12}=4.2$ Å. Thin line, solutes 1 and 2; dotted line, solute 3 (uncharged); broken line, solute 3 (positively charged); continuous line, solute 3 (negatively charged). Note that the Fourier spectrum of SIFs on solutes 1 and 2 is not affected by the presence and sign of the unit charge on solute 3. The progressively higher resolution of the peak reflects a progressively increasing, local oscillatory character of motions, which agrees with the progressively higher localization of hydration molecules shown below. Bottom, solute-water correlation function for single solutes (dotted line, uncharged; broken line, positively charged; continuous line, negatively charged). The *r* variable is the distance between the center of our LJ solute and the oxygen on the water molecules.

tively or negatively charged, respectively, while solute 2 is uncharged in all cases. Data relative to solute 1 are shown for this case in the left panel and, on a more expanded scale, in the center panel of the top row. Data relative to solute 2 are shown in the right panel of the same row. A similar presentation of data for the three-solute configuration is given in the same figure, bottom row. The left and central panels are relative to solute 3 and the right panel is relative to either solute 1 or 2. We see again in all cases the remarkable increase of τ_{res} in the hydration shell of the negatively charged solute. We also see that in all cases the presence of a negative solute also raises the τ_{res} values relative to the partner solute(s). Interestingly, in the two-solute case, at the $R_{12}=5.7$ Å distance corresponding to a maximum of the repulsive SIF acting between the two solutes (see Fig. 2 and Ref. [14]), the residence time shows a large and sharp maximum. For this particular situation, a view similar to that of Fig. 7, bottom (not shown), shows the presence of one water molecule trapped for long times (of the order of 100 ps) in the region of hydration overlap, and thus only occasionally exchanged. In summary, the data in Fig. 8 illustrate the context dependence (that is, the dependence on the presence of other nearby solutes) of the diffusional properties of hydration water.

Finally, in Fig. 9 the τ_{res} data of Fig. 8 are plotted along with the solvent contribution, Ψ, to PMF data already shown in Fig. 3. Both quantities refer to the solute configuration of Fig. 1 and concern the two LJ solutes 1 and 2, under the perturbation of solute 3 (absent, uncharged, positively, and negatively charged, respectively). The vertical scale of the τ_{res} data has been adjusted, so as to optimize the visualization of possible correlations between the two sets of data. Of course, this type of comparison is of qualitative and even uncertain meaning. All the same, we can infer from the figure a tendency towards a certain correlation between τ_{res} and Ψ. At first sight, the opposite behavior would be predicted, on the argument that longer-lived (more stable) water configurations would correspond to minimal PMF contribution. The observed opposite behavior suggests that a maximum of Ψ may correspond to a minimum entropy, implied by a scarce multiplicity of configurations accessible to the solvent and compatible with the solutes in the given configuration.

IV. COMMENTS AND CONCLUSIONS

We have used an explicit molecular solvent and modeled solutes as polar spheres to which a unit charge of either sign can be added in their geometric center. This has allowed eliciting perhaps at the simplest level and *ceteris paribus* the effect of charges on hydrophobic interactions and their microscopic origin. Data on hydration and on its dynamic properties provide a clue for understanding the weakening or even disruptive effect of charged solutes on hydrophobic bonds and its charge sign dependence. As seen in Fig. 6, the first and second peak of the solute-oxygen correlation function are, in the case of negatively charged solute, much higher and sharper, and occur at closer distance. This is because [13,14] the off-centered hydrogen atoms of the water molecule, pointing towards the negative solute, can reach closer to it than the negative oxygen of water in the case of the positive solute. The tightly bound and longer-lived hydration shells of the negatively charged solute are expected to be hardly compatible with optimal (''straddled H bond'') configurations of water molecules around hydrophobic solutes, and to have a consequent disturbing (or even disruptive) effect on them. The observed changes of SIFs and PMF appear to be a straightforward consequence of this disturbance. Correlation functions also reveal that, in the case of a positively charged solute, as a consequence of the weaker solute-water interaction, hydration shells are not as sharply defined, and they extend to a larger distance. For this reason, the positively charged solute has a weaker disruptive effect

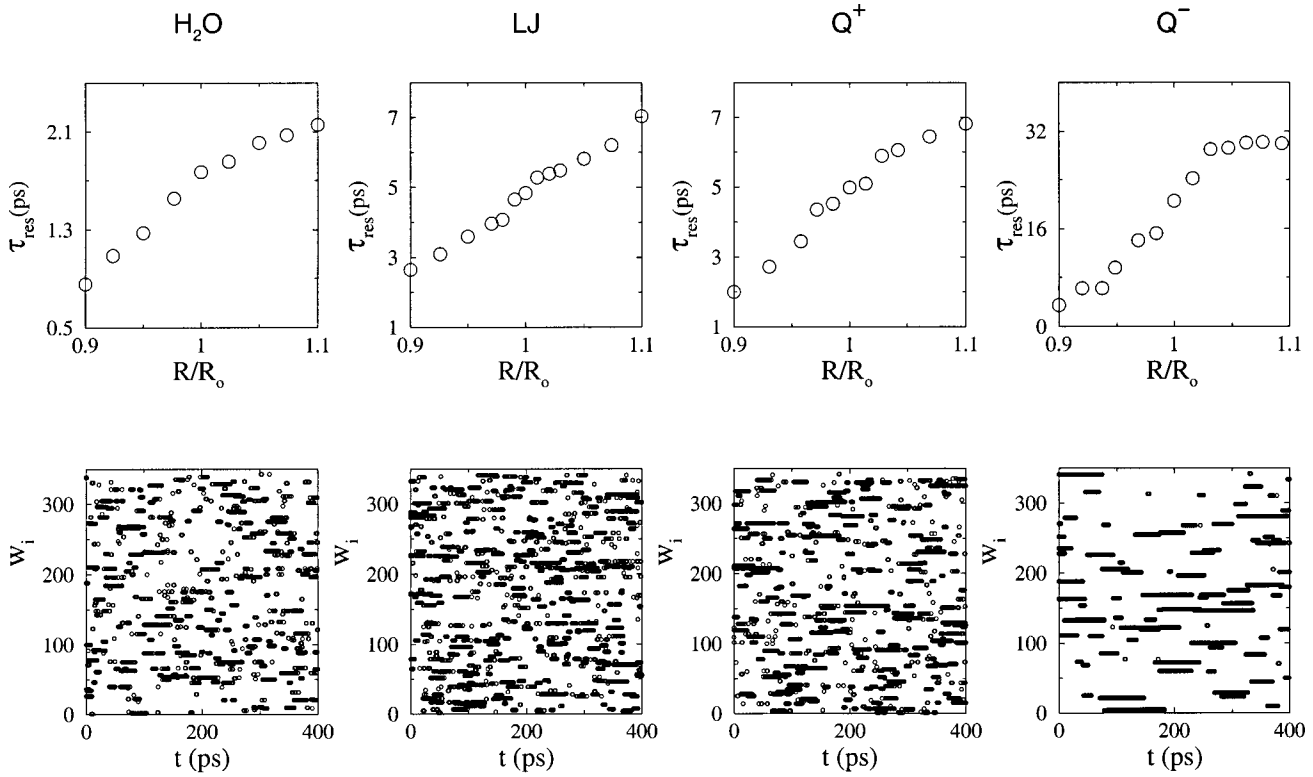

FIG. 7. Residence time (as defined in Sec. II) of water molecules in the first hydration shell of one single solute in a water bath. Left, around a free water molecule; center-left, around one single, fixed and uncharged solute; center-right, same fixed solute, positively charged; right, same, negatively charged. Top, residence time data are presented as a function of the chosen cutoff for the first hydration shell, R, normalized to the first minimum of the correlation function, R_0. Values of R_0, given by the $g(r)$ in Fig. 6, bottom, are 5, 3.6, and 3.25 Å, for uncharged, positively, and negatively charged solutes, respectively. Note the large-scale change of residence time on going from bulk water to uncharged and positively charged solutes to the negatively charged one. Bottom, for each water molecule (numbered by w_i), a circle is drawn when the given molecule is present in the first hydration shell (cutoff distance $R=R_0$). In this way, the average length of (apparently) continuous lines represents the average residence time spent in the hydration shell by the water molecule whose number, w_i, can be read on the ordinate axis.

on the hydrophobic attraction, which however, extends to a larger distance. As a consequence, the integrated effect on the PMF at $R_{12}>11$ Å is appreciably larger. The similar but smaller effect of the uncharged solute can be similarly understood.

Since these effects are essentially related to the overlap of hydration regions [25], a dependence on the h distance (see Fig. 1) is expected. This was in fact shown by data in Ref. [14], which refer to two h values and include the repulsive force acting on solute 3 (when charged). A prediction of the general trend can be given in thermodynamic terms and on the grounds of the present basic paradigmatic information. Water structural rearrangements and related free-energy changes caused by adding either one more solute element or an electric charge to a preexisting spatial context of simple elements imply a drive towards a new stable configuration of the system of solutes. In the configuration chosen for the present study, the ''hydrophobic contact bond'' is disrupted and generalized thermodynamic forces are expected to drive the system towards a new rearranged configuration of its solute elements. Since the free energy can be lowered if the third charged solute is brought to a large distance and the hydrophobic bond is reestablished, we expect (although in average only) a repulsive SIF acting on solute 3. This prediction agrees with the well-known effect of the exclusion of salts from apolar solutes [33].

Of course, in more realistic and complex systems, immensely richer situations are found. This is already evident in the still simple case of a somewhat larger number of solute elements [13]. In such a case, the same mechanism discussed here causes a weakening of the attractive SIFs between hydrophobic elements close to the charged ones. Further, repulsive SIFs act so as to push the charged element away from the apolar ones and to push those apolar elements which are closest to the charge towards more distant ones [13]. The same mechanism operates when charged and apolar solutes are free to diffuse in the solution [8], and it is the basis of the complex phenomenon of salting-out, that is, of the promotion of protein coagulation by salts [33,34].

Another charge-sign-dependent phenomenon elicited in the present work concerns the markedly different residence times of water molecules in the first hydration shell. Again, this can be traced to the difference between interactions of negative and positive solutes with water. Our data can be profitably put in relation to experimentally measured residence times of hydration water of anions and cations, available in the literature [35]. Interpretation of the latter is usually difficult because of the concurrent effects of ion size and charge sign, unavoidable in real experiments. However, when these data are plotted versus ion size [36], as in Fig. 10, the effects of charge sign and size are clearly distinguish-

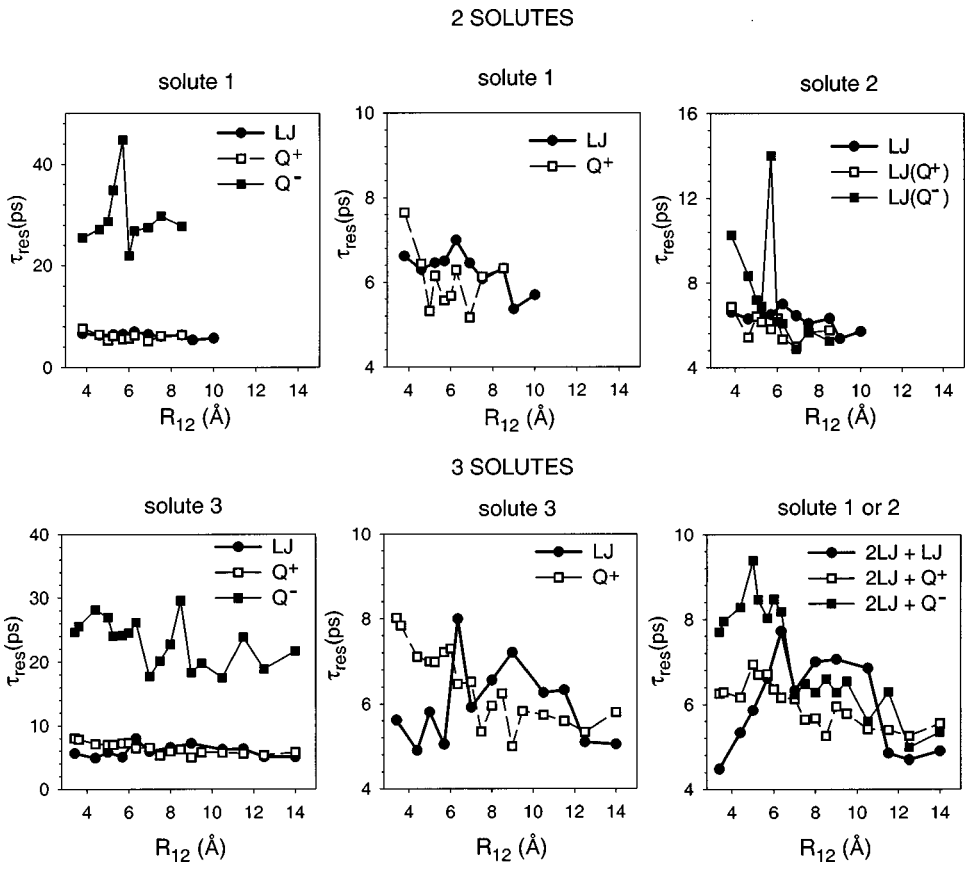

FIG. 8. Residence times of water molecules in the first hydration shell (cutoff $R=R_0$) of solutes of the same type as in Fig. 1 in a water bath, vs their R_{12} center-to-center distance. Top row, solute 3 is absent, and solute 1 bears a positive (empty squares), negative (full squares), or null (full circles) electric charge. Residence times of hydration water around solute 1 (left and center) and around solute 2 (right). Bottom row, three solutes in the configuration shown in Fig. 1. Residence time of hydration water around solute 3 (left and center) and around solutes 1 or 2 (right), for different charges on solute 3. Note the largely different scales in the left and right panels. The two center panels show details from data of the left panel, on an expanded scale.

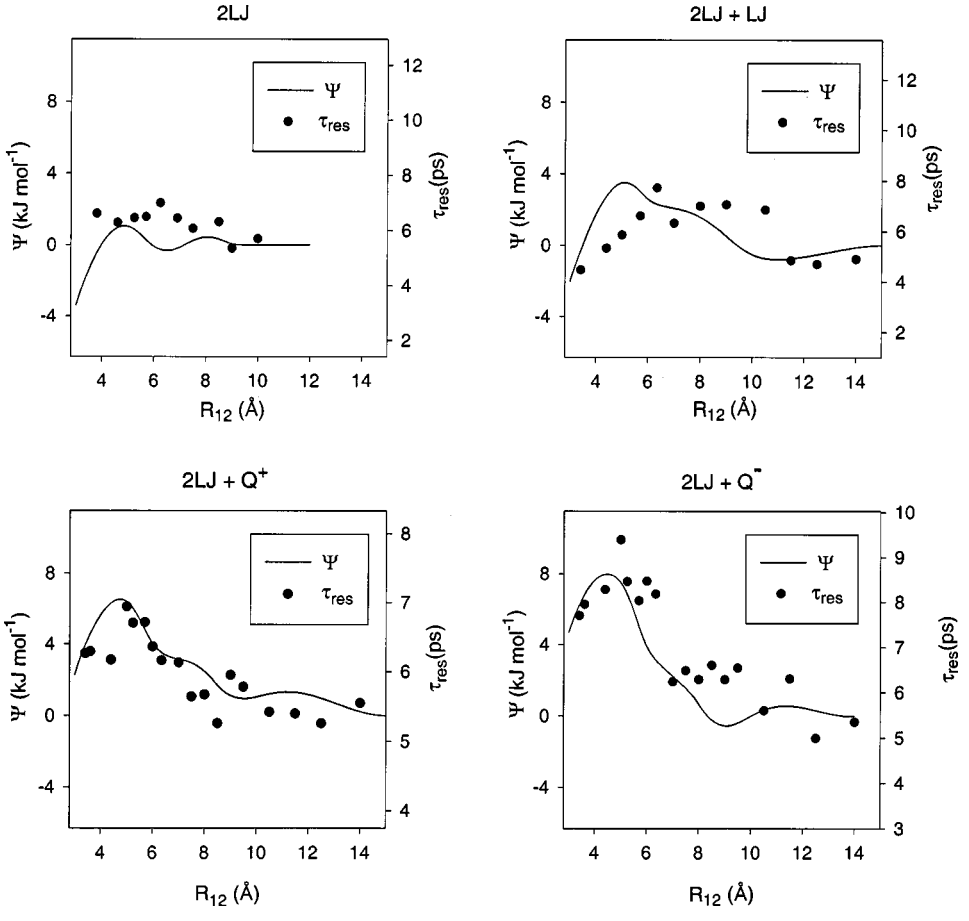

FIG. 9. Solvent contribution to PMF, Ψ, and residence time for the solute configuration of Fig. 1. Top left, solute 3 absent; top right, solute 3 uncharged; bottom left, solute 3 positively charged; bottom right, solute 3 negatively charged. Scales were optimized to visualize possible correlations between the dependence of Ψ and τ_{res} upon R_{12}.

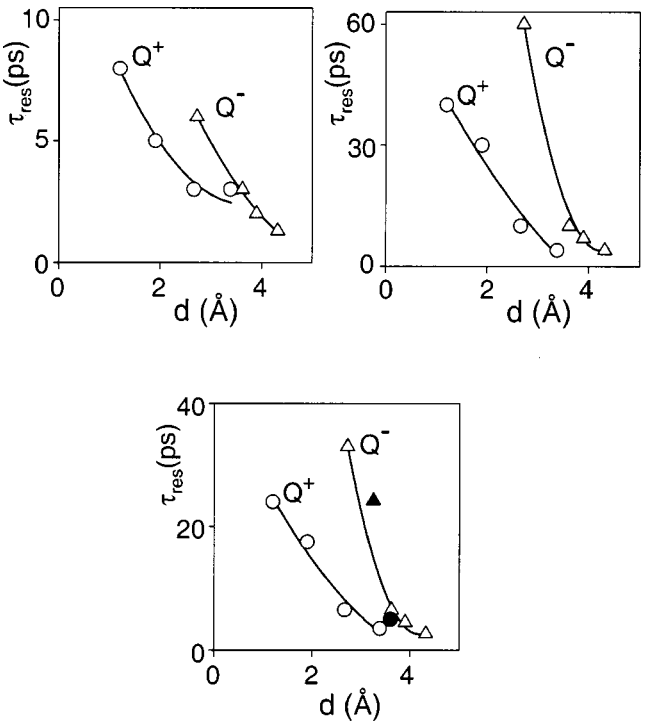

FIG. 10. Experimentally measured residence times (from Ref. [35]) for cations and ions vs ion diameter (from Ref. [36]). Due to the ample scatter of experimental data, we have plotted the minimum (top, left), maximum (top, right), and mean experimental values (bottom). Empty circles (in order of increasing size): Li^+, Na^+, K^+, Cs^+. Empty triangles (in order of increasing size): F^-, Cl^-, Br^-, I^-. Full circle and triangle: data from the present work, for negative and positive solute, respectively. The close numerical agreement of experimental and present data has to be taken as partially fortuitous. Note that curves relative to anions lay, for each set of data, well above those relative to cations, in full agreement with the present results.

able. Due to the large scatter of data, we show three different plots, for the minimum, mean, and maximum values, respectively. In all cases the charge sign dependence is clearly apparent. Curiously, data of the present work fall very close to the mean value lines relative to anions and cations, respectively. Such a close numerical agreement has to be seen as fortuitous to a large extent considering the large scatter of experimental data and the uncertainties intrinsically present in simulation work. This notwithstanding, the agreement with the size of the charge sign dependence provides rewarding support of the validity of the present results and an explanation on microscopic bases of the experimental data.

Further, it is worth noting that, due to the intense local electric field, water molecules in the hydration shells of charged solutes are not expected to form a net of regular water-water hydrogen bonds. Electrostriction explains the tight packing revealed by the high peak in the correlation function, the more so in the case of the negative solute. This tight packing and the related increase of local density are similar to that caused by high pressure. This is shown by recent neutron-scattering experimental findings [27] eliciting a quantitative correspondence between the effects of salts and those of high pressure on local density and structure of solvent water. In the experimental case, however, the neutrality of the solution prevents revealing the charge sign dependence observed in simulations.

Finally, we note the relation of our results to the actual cases of ubiquitous biological processes such as phosphorilation and methylation and the consequent drive towards functional changes of biomolecular conformation. The common feature of all these cases is that, by the same mechanism, the arrival of a new charged solute element can drive the system in a sufficiently energetic way towards a configurational change, by way of solvent-induced interactions. This does not prove, of course, that solvent-induced interactions are the sole responsible for the drive towards actual biomolecular conformational changes caused by the arrival of a new (either apolar or charged) solute element such as in phosphorilation and methylation. However, the size of the effects elicited at the present basic level evidence how solvent-induced interactions can have an important and even overwhelming role in such conformational changes.

The conceptual distance between these complex phenomena and the case of our system of simple solute elements is shorter than one would expect at first sight. This can be appreciated by considering that, as remarked by Delbruck, the vastness and complexity of real-life phenomena may hinder the progress from a ''semidescriptive'' understanding to a ''radical'' one based on the laws of physics [37]. Looking for such a desirable radical physical explanation requires using drastic simplifications that are still capable of capturing the physical essence of the phenomena being studied. For this reason and at variance with other methods focusing on larger-scale (average) features, we have taken the complementary approach of using a minimal number of simple solutes. The strong simplification enables us to elicit the detailed grounds for the wanted physical understanding and the high local specificity, which is a central feature of biomolecular function.

ACKNOWLEDGMENTS

Long-term collaboration and discussions with M. U. Palma, S. L. Fornili, and A. Emanuele are gratefully acknowledged.

[1] H. S. Frank and M. W. Evans, J. Chem. Phys. **13**, 507 (1945).
[2] W. Kauzmann, Adv. Protein Chem. **14**, 1 (1959).
[3] F. Franks, in *Water: A Comprehensive Treatise*, edited by F. Franks (Plenum, New York, 1975), Vols. 2 and 4.
[4] F. H. Stillinger, Science **209**, 451 (1980); A. Geiger, A. Rahman, and F. H. Stillinger, J. Chem. Phys. **70**, 263 (1979); D. A. Zichi and P. J. Rossky, *ibid.* **83**, 797 (1985).
[5] K. A. Dill, Biochemistry **29**, 7133 (1995).
[6] L. Pratt and D. Chandler, J. Chem. Phys. **73**, 3434 (1980); C. Pangali, M. Rao, and B. J. Berne, *ibid.* **71**, 2975 (1982); **71**, 2982 (1982); G. Ravishanker, M. Mezei, and D. L. Beveridge, Faraday Symp. Chem. Soc. **17**, 79 (1982); S. Lüdemann, H. Schreiber, R. Abseher, and O. Steinhauser, J. Chem. Phys. **104**, 286 (1996).

[7] L. A. Kuhn, M. A. Siani, M. E. Pique, C. L. Fisher, E. D. Getzoff, and J. A. Tainer, J. Mol. Biol. **228**, 13 (1992); H. S. Chan and K. A. Dill, J. Chem. Phys. **101**, 7007 (1994); A. Wallqvist and B. J. Berne, J. Phys. Chem. **99**, 2893 (1995); Y. K. Cheng and P. J. Rossky, Nature (London) **392**, 696 (1998); Biopolymers **50**, 742 (1999).

[8] R. L. Mancera, Chem. Phys. Lett. **296**, 459 (1998); J. Phys. Chem. B **103**, 3774 (1999); P. E. Smith, *ibid.* **103**, 525 (1999).

[9] P. K. Murphy, P. L. Privalov, and S. J. Gill, Science **247**, 559 (1990); J. R. Livingstone, R. S. Spolar, and M. T. Record, Jr., Biochemistry **30**, 4237 (1991).

[10] D. Bulone, M. B. Palma-Vittorelli, and M. U. Palma, Int. J. Quantum Chem. **42**, 1427 (1992); D. Bulone, P. L. San Biagio, M. B. Palma-Vittorelli, and M. U. Palma, Science **259**, 1335 (1993).

[11] F. Brugè, S. L. Fornili, G. G. Malenkov, M. B. Palma-Vittorelli, and M. U. Palma, Chem. Phys. Lett. **254**, 283 (1996).

[12] V. Martorana, G. Corongiu, and M. U. Palma, Chem. Phys. Lett. **254**, 292 (1996); V. Martorana, G. Corongiu, and M. U. Palma, Proteins: Struct., Funct., Genet. **32**, 129 (1998).

[13] V. Martorana, D. Bulone, P. L. San Biagio, M. B. Palma-Vittorelli, and M. U. Palma, Biophys. J. **73**, 31 (1997); P. L. San Biagio, D. Bulone, V. Martorana, M. B. Palma-Vittorelli, and M. U. Palma, Eur. Biophys. J. **27**, 183 (1998).

[14] D. Bulone, V. Martorana, P. L. San Biagio, and M. B. Palma-Vittorelli, Phys. Rev. E **56**, R4939 (1997).

[15] J. G. Kirkwood, J. Chem. Phys. **3**, 300 (1935); T. L. Hill, *Statistical Mechanics* (Dover, New York, 1956).

[16] B. M. Pettitt, M. Karplus, and P. J. Rossky, J. Phys. Chem. **90**, 6335 (1986); C. V. Valdeavella, J. S. Perkyns, and B. M. Pettitt, J. Chem. Phys. **101**, 5093 (1994); J. S. Perkyns and B. M. Pettitt, J. Phys. Chem. **99**, 1 (1995).

[17] A. Kitao, F. Hirata, and N. Gō, Chem. Phys. **158**, 447 (1991).

[18] R. Klement, D. M. Soumpasis, and T. M. Jovin, Proc. Natl. Acad. Sci. U.S.A. **88**, 4631 (1991); S. Garde, G. Hummer, A. F. Garcia, L. R. Pratt, and M. B. Paulaitis, Phys. Rev. E **53**, R4310 (1996); G. Hummer, A. F. Garcia, and D. M. Soumpasis, Faraday Discuss. **103**, 175 (1996).

[19] M. Pellegrini and S. Doniach, J. Chem. Phys. **103**, 2698 (1995).

[20] For useful comparative discussions of different solvent modeling, see A. Rashin, J. Phys. Chem. **93**, 4664 (1989); G. King, F. S. Lee, and A. Warshel, J. Chem. Phys. **95**, 4366 (1991); L. R. Pratt, G. Hummer, and A. F. Garcia, Biophys. Chem. **51**, 147 (1994); F. E. Figuerido, G. S. Del Buono, and R. M. Levy, *ibid.* **51**, 253 (1994); Y. Marcus, *ibid.* **51**, 111 (1994); P. E. Smith and B. M. Pettitt, J. Phys. Chem. **98**, 9700 (1994).

[21] C. B. Anfinsen, Science **181**, 223 (1973).

[22] P. L. San Biagio, V. Martorana, D. Bulone, M. B. Palma-Vittorelli, and M. U. Palma, Biophys. J. **77**, 2470 (1999); A. C. Vaiana and M. B. Palma-Vittorelli, in *Nuclear and Condensed Matter*, edited by A. Messina, AIP Conf. Proc. No. 513 (AIP, New York), p. 238.

[23] A. P. Pertsemlidis, A. M. Saxena, A. K. Soper, T. Head-Gordon, and R. M. Glaeser, Proc. Natl. Acad. Sci. U.S.A. **93**, 10 769 (1996); A. Pertsemlidis, A. K. Soper, J. M. Sorenson, and T. Head-Gordon, *ibid.* **96**, 481 (1999).

[24] B. M. Pettitt and P. J. Rossky, Isr. J. Chem. **27**, 156 (1986); B. Roux, H. A. Yu, and M. Karplus, J. Phys. Chem. **94**, 4683 (1990); H. Ohtaki and K. Heinzinger, in *Structure and Dynamics of Solutions*, edited by H. Ohtaki and H. Yamatera (Elsevier Science, Amsterdam, 1992); S. Rick and B. J. Berne, J. Am. Chem. Soc. **116**, 3949 (1994); S. Garde, G. Hummer, and M. E. Paulaitis, J. Chem. Phys. **108**, 1552 (1998).

[25] S. Lifson and I. Oppenheim, J. Chem. Phys. **33**, 109 (1960).

[26] F. Brugè, S. L. Fornili, and M. B. Palma-Vittorelli, J. Chem. Phys. **101**, 2407 (1994); F. Brugè, G. Cottone, R. Noto, and S. L. Fornili, J. Chim. Phys. Phys.-Chim. Biol. **93**, 1858 (1996).

[27] R. Leberman and A. K. Soper, Nature (London) **378**, 364 (1995).

[28] D. Bulone, C. Spinnato, F. Madonia, and M. U. Palma, J. Chem. Phys. **91**, 408 (1989); D. Bulone, I. D. Donato, M. B. Palma-Vittorelli, and M. U. Palma, *ibid.* **94**, 6816 (1991).

[29] W. L. Jorgensen, J. Chandrasekhar, D. J. Madura, R. W. Impey, and M. L. Klein, J. Chem. Phys. **79**, 926 (1983).

[30] G. Corongiu and V. Martorana, in *Metecc-94*, edited by E. Clementi (STEF, Cagliari, 1993), p. 81.

[31] F. Brugè, E. Parisi, and S. L. Fornili, Chem. Phys. Lett. **250**, 443 (1996); A. F. Garcia and L. Stiller, J. Comput. Chem. **14**, 1396 (1993).

[32] I. Ohmine and H. Tanaka, Chem. Rev. **93**, 2545 (1993); D. J. Wales and I. Ohmine, J. Chem. Phys. **98**, 245 (1993); **98**, 7257 (1993).

[33] T. Arakawa and S. N. Timasheff, Biochemistry **21**, 6545 (1982); **23**, 5912 (1984).

[34] F. Hofmeister, Arch. Exp. Path. Pharmakol. **24**, 247 (1888).

[35] P. Bopp, in *The Physics and Chemistry of Aqueous Ionic Solutions*, edited by M. C. Bellissant-Funel and G. W. Neilsen (Reidel, Dordrecht, The Netherlands, 1987), p. 217; G. Jancsò, P. Bopp, and K. Heinzinger, Hungarian Academy of Sciences, Report No. KFKI-1977-101 1977.

[36] *CRC Handbook of Chemistry and Physics*, edited by D. R. Lide (CRC, Boca Raton, FL, 1995); L. Pauling, *Nature of the Chemical Bond* (Cornell University Press, Ithaca, NY, 1960).

[37] M. Delbruck, Trans. Conn. Acad. Arts Sci. **38**, 173 (1949); H. Varmus, Phys. World **12** (9), 27 (1999).